1-19-2008

Gd-doping of HfO_2

Ihor Ketsman
University of Nebraska-Lincoln, iketsman@gmail.com

Yaroslav B. Losovyj
University of Nebraska-Lincoln, ylozovyy@indiana.edu

Jinke Tang
University of Wyoming, jtang2@uwyo.edu

Zhenjun Wang
University of Wyoming

M. L. Natta
University of Nebraska-Lincoln

See next page for additional authors

Published in *Applied Surface Science* (2008); doi:10.1016/j.apsusc.2008.01.060

Published online January 19, 2008.

Gd-doping of HfO_2

Ihor Ketsman [1], Ya. B. Losovyj [1, 2], A. Sokolov [1], Jinke Tang [3], Zhenjun Wang [3], M. L. Natta [4], J. I. Brand [4], and P.A. Dowben [1]

[1] Department of Physics and Astronomy and the Nebraska Center for Materials and Nanoscience, University of Nebraska–Lincoln, P.O. Box 880111, Lincoln, NE 68588-0111, USA

[2] Center for Advanced Microstructures and Devices, Louisiana State University, 6980 Jefferson Highway, Baton Rouge, LA 70806, USA

[3] Department of Physics and Astronomy, University of Wyoming, Laramie, WY 82071, USA

[4] College of Engineering and Technology, and the Nebraska Center for Materials and Nanoscience, N209 Walter Scott Engineering Center, 17th & Vine Streets, University of Nebraska–Lincoln, Lincoln, Nebraska 68588-0511, USA

Corresponding author: Ihor Ketsman

Abstract

An increase in the density of states between the oxygen 2p bands and the Fermi level is seen with increasing Gd concentrations. In addition, for the Gd-doped HfO_2 films, the Gd 4f photoexcitation peak at 5.5 eV below the valence band maximum was identified using resonant photoemission. Electrical measurements show pronounced rectification properties for lightly-doped Gd:HfO_2 films on *p*-Si and for heavily-doped Gd:HfO_2 films on *n*-Si, suggesting a crossover from *n*-type to *p*-type behavior with increasing doping level. In addition, there is an increase in the reverse bias current with neutron irradiation.

Keywords: oxide dielectric layers, hafnium oxide, Gd doping, resonant photoemission

PACS classification codes: 79.60.Jv; 68.55.Ln; 29.40.Wk; 81.05.J

1. Introduction

While HfO_2 has attracted considerable attention as a high-κ dielectric oxide [1–3], the gadolinium doping of a number of wide band gap semiconductors [4–8] suggests that Gd doping of HfO_2 may also lead to a dilute magnetic semiconductor [9, 10]. With increased Gd-doping concentrations there is a shift from monoclinic phase so that Gd_2O_3-doping stabilizes HfO_2 in the cubic phase [11–14], which may possibly be a better semiconductor. Moreover, semiconducting Gd-doped HfO_2 may provide a promising new class of materials for neutron detection technologies.

A gadolinium-based semiconductor diode might be better for neutron detection because of the large thermal neutron absorption cross-section of gadolinium (on average ~46,000 barns). The $^{157}Gd(n,\gamma) \rightarrow {}^{158}Gd$ and $^{155}Gd(n,\gamma) \rightarrow {}^{156}Gd$ reactions lead to the emission of low-energy gamma rays and conversion electrons, most of which are emitted at energies below 220 eV [15–18]. The creation of conversion electrons is the result of the de-excitation of the ^{158}Gd and ^{156}Gd nuclei through lower level nuclear states where internal conversion occurs and conversion electrons and low-energy X-rays are released. The appeal of using ^{157}Gd is due to its large thermal neutron cross-section of 240,000 barns [19, 20]. Although sensitive to gamma radiation, the big advantage of gadolinium over boron is not only the high neutron capture cross-section but that this cross-section extends to higher neutron energies (200 meV) than in the case for boron. While all boron carbide neutron detectors have been demonstrated [21–23], and their potential detection efficiency is much higher than that of many semiconductor materials (likely well above 50% for ^{10}B enriched devices), the drawback to all boron-based devices is the need for a moderator to reduce the neutron kinetic energies to 25–30 meV. Fissile radiation sources like ^{235}U or ^{239}Pu produce 1–2 MeV neutrons, so the moderator must be significant.

Since neutron capture by gadolinium leads to production of conversion electrons, the pulse height will be smaller than in the case of neutron capture by boron (10^4 charges

versus 10^6 per neutron capture). Accordingly, it is advantageous to see if a Gd-doped HfO_2 diode can be fabricated that can be impedance matched and compatible with a high gain, low noise amplifier. A heterojunction diode with silicon would serve this purpose.

2. Experiment

The Gd-doped HfO_2 films were deposited on both *p*-type and *n*-type single crystal Si(1 0 0) substrates using pulsed laser deposition (PLD) at a growth rate of about 0.15 Å/s. The Gd-HfO_2 target was prepared by standard ceramic techniques using HfO_2 and Gd_2O_3 powders, as described elsewhere [10, 14, 24]. Before the deposition, the Si(1 0 0) substrates were cleaned with diluted HF acid, rinsed with acetone, and then immediately put in vacuum chamber. Before deposition, the surface of Si wafer was sputter cleaned in a plasma of H_2 (8%) and Ar (92%) mixture created by a DC sputtering gun operating in the reverse bias mode. The films were deposited at a substrate temperature of 500 °C. The deposition was carried out in a mixture of H_2 and Ar (8% H_2) to introduce oxygen vacancies, and the vacuum was maintained at 10^{-5} Torr during the deposition. The doping level was estimated from the target composition and confirmed by performing near edge X-ray absorption spectroscopy (NEXAFS) and by X-ray emission spectroscopy (XES or EDAX) on separate similarly prepared samples (Throughout, *x*% Gd means the nominal composition $Hf_{1-x}Gd_xO_{2-0.5x}$). The complementary spectroscopies show that the films and the target have essentially the same composition. The NEXAFS and EXAFS data indicate that the Gd atoms occupy the Hf sites in the Gd-doped HfO_2 films.

X-ray diffraction (XRD) patterns show that the HfO_2 films with 3% Gd, which are approximately 250 nm thick, are in the single monoclinic phase with strong texture growth and about 3% strain compared to the undoped HfO_2 [10, 14, 24]. It has been estimated that the spacing of the (−1 1 1) lattice planes increased by $d = 0.0030$ nm, from 0.3147(1) nm for 0% Gd to 0.3177(1) nm for 3% Gd [10, 24]. With increased doping levels, the fcc fluorite phase becomes dominant over the monoclinic phase, as expected [11–14] (although the presence of a small amount of the $Gd_2Hf_2O_7$ pyrochlore phase cannot, *a priori*, be excluded). For the 10% Gd-doping level, the film is largely in the new fluorite phase but retains a minority monoclinic phase component. For 15% Gd doping, however, the films are free of the monoclinic phase, i.e. no minority monoclinic phase is observed [14].

To determine the position of the Fermi level, angle-resolved photoemission experiments were performed using the 3 m toroidal grating monochromator (3 m TGM) beam line in a UHV chamber previously described [24, 25]. The Fermi level (E_F) was established from a gold film in electrical contact with the sample and measurements were carried out at ambient temperatures. Photoemission was undertaken over a range of temperatures from 100 to 700 K, but the data presented here was taken at 320 °C, where surface charging was found to be negligible. Both NEXAF and the phase diagram [11–13] indicate there is very little change in the bulk structure at this temperature, as our studies are taken well below the temperature dependent structural phase transition (700 °C).

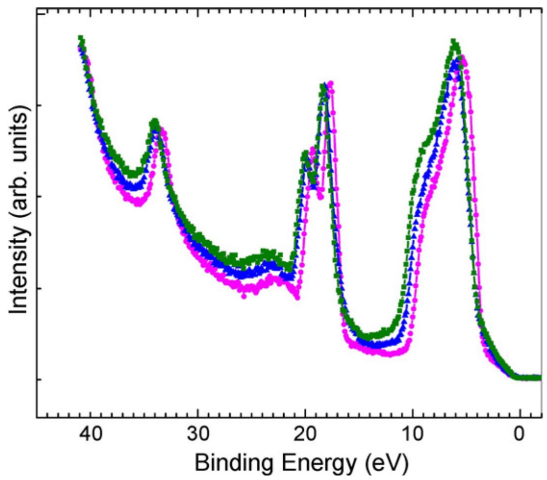

Figure 1. Different bands intensities for: pristine 0% (purple circles), 3% (blue triangles), 15% (green squares) Gd-doped films of HfO_2. The photon energy is 70 eV and the light incidence angle is 45°. All photoelectrons were collected along the surface normal at $T = 320$ °C.

3. The occupied density of states with Gd doping

From Figure 1, it is clear that the nominal valence band edge is placed well away from the Fermi level for both Gd-doped and undoped HfO_2 films. The Hf 4f binding energies, at 18–21 eV binding energy, are substantially larger than those reported by Renault et al. [26], and Hf 4f binding energies and valence band edge are slightly larger than those reported elsewhere [27–29]. Indeed, with Gd doping, the Hf 4f binding energies increase, as seen in Figure 1. The increase with Gd doping in the intensity of the photoemission features in the oxygen 2p region of the valence band, at 5–10 eV binding energy, relative to the Hf 4f features at 18–21 eV binding energies, suggests that there are Gd 4f contributions to these largely O 2p dominated lower binding energy features, as is expected from studies of HfO_2-Y_2O_3 composite films [30]. In Figure 1 and Figure 2, one can clearly see a shoulder on the broad photoemission peak at the binding energy of 9–10 eV. In order to assist in the identification of this feature, we performed resonant photoemission (i.e. constant initial state spectroscopy) measurements; the results are shown in Figure 2.

The photoelectron intensity, determined from the feature at about 9.5 eV binding energy (from the Fermi level), is strongly enhanced at about 148 eV photon energy. This resonant enhancement has been plotted for various photon energies, as shown in the inset to Figure 2. It is clear that the resonant enhancements in the photoemission intensity, from this 9.5 eV binding energy final state, occur at photon energies corresponding to the binding energy of the Gd $4d_{3/2}$ (147 eV) shallow core. Thus, this feature at 9.5 eV binding energy has strong Gd weight, and the resonant photoemission process occurs because of an excitation from the 4d cores to a bound state, but with a final state identical to that resulting from direct photoemission from Gd 4f

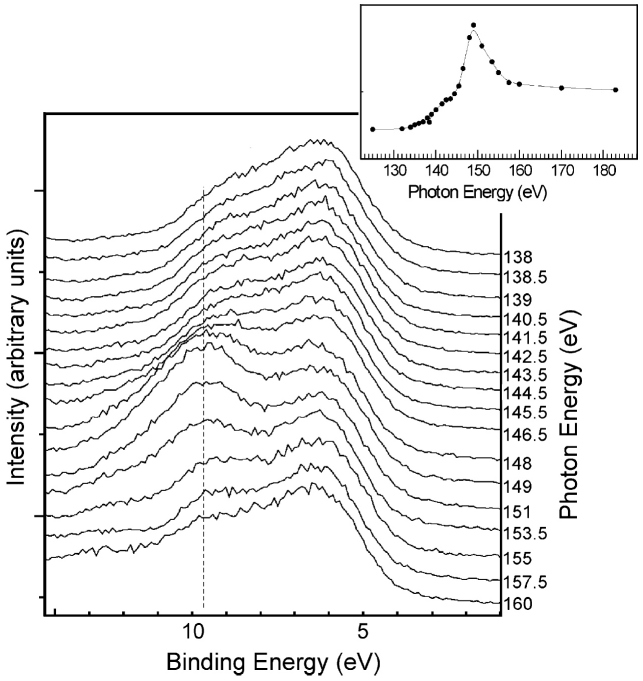

Figure 2. Resonant photoemission for Gd-doped films of HfO_2. Light incidence angle is 45°. All photoelectrons were collected along the surface normal.

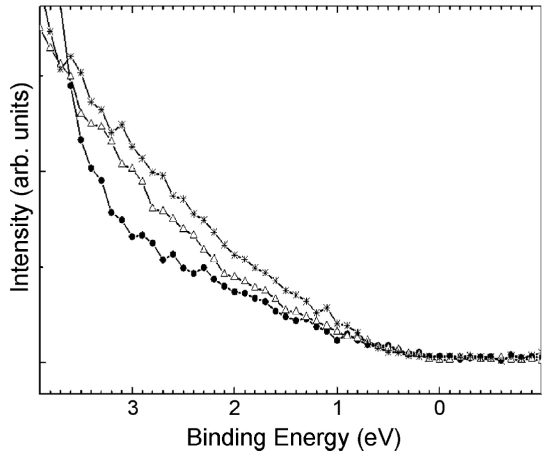

Figure 3. The increasing contributions to the density of states near to the Fermi level are illustrated for 0% (black dots), 3% (open triangles), and 15% (stars) Gd doping levels.

states [31–33], that is to say is due to constructive interference between the direct 4f photoionization and a $4d^{10}4f^7 \rightarrow 4d^94f^8 \rightarrow 4d^{10}4f^6 + e^-$ super Coster-Kronig transition [32], leading to a classic Fano resonance. From the 4f-hole calculations [14, 24], we have obtained the Gd-4f binding energy of about 5.5 eV below the valence band maximum, which is in excellent agreement with the photoemission data.

With Gd doping, there is also an increase in the small density of states between 4 eV binding energy and the Fermi level, as seen in Figure 3. In this region, the density of states measured by photoemission decrease with increasing yttrium-doping levels [30], but is seen here to increase with Gd doping. Indeed, the increase in binding energy of all the major photoemission features seen with Gd doping is not observed for $(HfO_2)_{1-x}(Y_2O_3)_x$ samples [30]. The possibility of surface defects or surface states pinning the Fermi level differently for the two different dopants (Y and Gd) cannot be excluded and may in fact be likely. Yttrium segregates away from the surface of zirconia [34], and may behave similarly with HfO_2, while gadolinium, because of its larger size, should segregate toward the surface; although for the samples studied here, significant gadolinium surface segregation was not observed. Thus, even with nominally similar surface terminations [35], the Fermi level pinning may be very different for the two dopants. States are added with increased Gd doping between the O 2p states and the Fermi energy as indicated in Figure 3. While Gd is expected to be a *p*-type dopant in HfO_2, the Gd acceptor states can be overcompensated by donor states introduced by oxygen vacancies [14, 24], as we note below.

4. Heterojunction rectification

We fabricated several diodes to illustrate that the overcompensation of the expected Gd acceptor states, by oxygen vacancies, as is seen with smaller (3 at.%) Gd doping levels [24] is not sustained at the higher Gd doping levels [14]. An *n*-type band offset of the lightly Gd-doped HfO_2 relative to *p*-type silicon is indicated by the excellent diode rectification seen for a heterojunction of 3% Gd-doped HfO_2 and *p*-type silicon, as shown in Figure 4. For the 10% Gd:HfO_2/*p*-Si heterojunction, no rectification or diode like characteristics are seen, but for the 10% Gd-doped HfO_2 to *n*-type silicon heterojunction, we do observe rectification or diode like characteristics, shown in Figure 4. While these data do not conclusively show the dominant carrier, they suggest that oxygen vacancies can overcompensate the Gd acceptor states without completely destroying the semiconductor properties for 3% Gd doping levels but not 10% Gd doping levels or higher.

Even with a heterojunction of 3% Gd-doped HfO_2 and *p*-type silicon, neutron absorption is indeed indicated. As seen in the upper right (first quadrant) of the diode curves in panel (a) in Figure 4, the reverse bias current increases under bright white light illumination and even further under irradiation from the combination of epithermal neutrons (600 neutrons/s cm^2) and gamma radiation from a fully moderated PuBe source [21, 22]. This increase in reverse bias current is not a demonstration of direct neutron detection, as (as indicated) this is somewhat akin to increased photoconductivity and not necessary directly related to either neutron or gamma capture and subsequent current generation. Nonetheless, given that the Gd doped hafnium oxide films are very thin, neutron capture is far more likely to be the origin of the increase in reverse bias current that gamma capture.

5. Summary

The data does show that such heterojunction devices have possible promise as neutron detectors. Even if such devices are successful as neutron detectors, distinguishing gamma and neutron adsorption will be problematic. A rare-earth (gadolinium) semiconductor heterostructure diode could

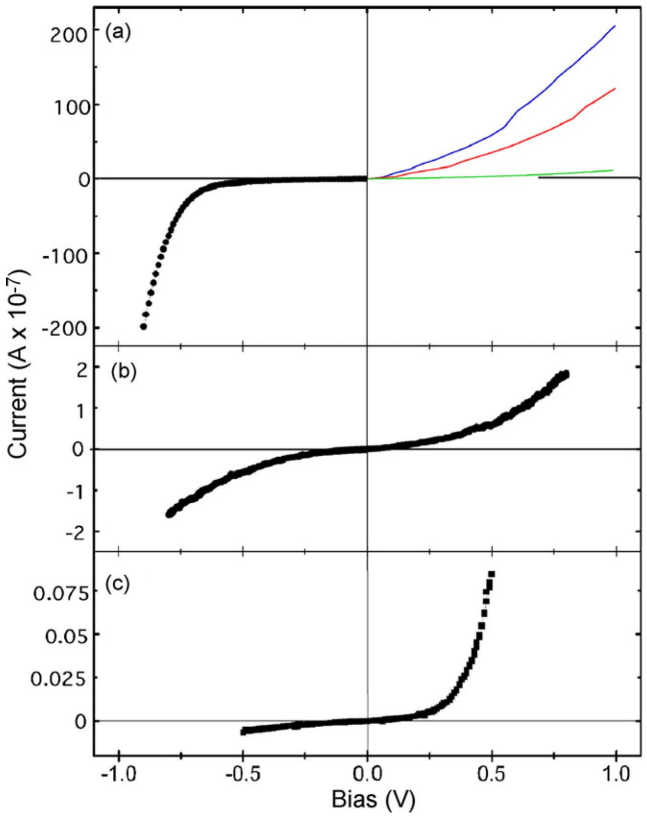

Figure 4. A heterojunction diodes constructed from Gd-doped HfO_2 on silicon, for various Gd-doping concentrations. With oxygen vacancies, the Gd doping generated acceptor states, in 3% Gd-doped HfO_2, are over compensated and doped hafnium oxide forms a rectifying diode on *p*-type silicon (a). The 10% Gd-doped HfO_2 is not overcompensated by oxygen vacancies and does not form a rectifying diode on *p*-type silicon (b) but does do so on *n*-type silicon (c). The increase in reverse bias current (green) for a 3% Gd-doped HfO_2 rectifying diode on *p*-type silicon (a), in the first quadrant of the inverted diode curve(s), illuminated with visible light (red) and with an incident neutron and gamma flux from a PuBe source (blue) is indicated

be formed with a boron rich semiconductor layer (e.g. boron carbide [21–23] or boron nitride [36]) layer as one side of the *p*–*n* junction and the rare-earth (gadolinium) semiconductor as the other side. Such a heterojunction would be much like the all boron carbide heterostructure [37], a boron carbide to silicon [38], or boron carbide to SiC heterojunction diode [39]. It may be possible, in such heterojunctions, to use the pulse height spectra to distinguish neutron capture events from other events, such as those resulting from gamma radiation.

The recognition of the value of a possible gadolinium-based semiconductor solid state detection of neutrons is not new: Aoyama et al. [40], and Mireshghi et al. [19], and many others have tried to incorporate boron and gadolinium in a neutron detector to increase the overall neutron capture ability of existing devices with varying results. With the development of a proper gadolinium containing semiconductor or even a gadolinium dielectric layer (suitable for a *p*–*i*–*n* heterojunction structure), one may be able to succeed, where prior efforts have been rather lack luster.

Acknowledgments

The authors acknowledge insightful discussions with David Wisbey, Andre Petuhkov, and K. Belashchenko. This work was supported by the Office of Naval Research (Grant No. N00014-06-1-0616), the Defense Threat Reduction Agency (Grant No. HDTRA1-07-1-0008), and the Nebraska Research Initiative.

References

[1] M. McCoy, *Chem. Eng. News* **83** (2005), p. 26.
M. McCoy, *Chem. Eng. News* **85** (2007), p. 10.

[2] B. H. Lee, L. Kang, W.-J. Qi, R. Nieh, K. Onishi, and J. C. Lee, *Tech. Dig.-Int. Electron Devices Meet.* **1999** (1999), p. 133.

[3] M. Gutowski, J. E. Jaffe, C.-L. Liu, M. Stoker, R. I. Hegde, R. S. Raj, and P. J. Tobin, *Appl. Phys. Lett.* **80** (2002), p. 1897.
K. P. Bastos, J. Morais, L. Miotti, R. P. Pezzi, G. V. Soares, I. J. R. Baumvol, R. I. Hegde, H. H. Tseng, and P. J. Tobin, *Appl. Phys. Lett.* **81** (2002), p. 1669.

[4] S. Dhar, O. Brandt, M. Ramsteiner, V. F. Sapega, and K. H. Ploog, *Phys. Rev. Lett.* **94** (2005), p. 037205.

[5] S. Dhar, L. Pérez, O. Brandt, A. Trampert, K. H. Ploog, J. Keller, and B. Beschoten, *Phys. Rev. B* **72** (2005), p. 245203.

[6] S. Dhar, T. Kammermeir, A. Ney, L. Pérez, K. H. Ploog, A. Melnikov, and A. D. Wieck, *Appl. Phys. Lett.* **89** (2006), p. 062503.

[7] L. Pérez, G. S. Lau, S. Dhar, O. Brandt, and K. H. Ploog, *Phys. Rev. B* **74** (2006), p. 195207.

[8] K. Potzger, S.-q. Zhou, F. Eichhorn, M. Helm, W. Skorupa, A. Mücklich, J. Fassbender, T. Herrmannsdorfer, and A. Bianchi, *J. Appl. Phys.* **99** (2006), p. 063906.

[9] M. Venkatesan, C. B. Fitzgerald, and J. D. M. Coey, *Nature* **430** (2004), p. 630.

[10] W. Wang, Y. Hong, M. Yu, B. Rout, G. A. Glass, and J. Tang, *J. Appl. Phys.* **99** (2006), p. 08M117.

[11] V. V. Kharton, A. A. Yaremchenko, E. N. Naumovich, and F. M. B. Marques, *J. Solid State Electrochem.* **4** (2000), p. 243.

[12] S. L. Dole, O. Hunter Jr., and F. W. Calderwood, *J. Am. Ceram. Soc.* **63** (1980), p. 136.

[13] S. V. Ushakov, A. Navrotsky, and K. B. Helean, *J. Am. Ceram. Soc.* **90** (2007), p. 1171.

[14] Ya. B. Losovyj, I. Ketsman, A. Sokolov, K. D. Belashchenko, P. A. Dowben, J. Tang, and Z. Wang, *Appl. Phys. Lett.* **91** (2007), p. 132908.

[15] K. S. Shah, L. Cirignano, R. Grazioso, M. Klugerman, P. R. Bennet, T. K. Gupta, W. W. Moses, M. J. Weber, and S. E. Derenzo, http://breast.lbl.gov/~wwwinstr/publications/Papers/LBNL-50253.pdf . (2001).

[16] S. F. Mughabghab, *Neutron Cross Sections* **vol. 1**, Academic Press (1981).

[17] P. L. Reeder, *Nucl. Instrum. Methods Phys. Res. A* **353** (1994), p. 134.

[18] B. Gebauer, Ch. Schulz, and Th. Wilpert, *Nucl. Instrum. Methods Phys. Res. A* **392** (1997), p. 68.

[19] A. Mireshghi, G. Cho, J. S. Drewery, W. S. Hong, T. Jing, H. Lee, S. N. Kaplan, and V. Perez-Mendez, *IEEE Trans. Nucl. Sci.* **41** (1994), p. 915.

[20] D. I. Garber and R. R. Kinsey (third ed.), *BNL:325 Neutron Cross Sections* **vol. 2**, Brookhaven National Laboratory, Upton (1976).

[21] A. N. Caruso, R. B. Billa, S. Balaz, J. I. Brand, and P. A. Dowben, *J. Phys.: Cond. Matter* **16** (2004), p. L139.

[22] A. N. Caruso, P. A. Dowben, S. Balkir, N. Schemm, K. Osberg, R. W. Fairchild, O. B. Flores, S. Balaz, A. D. Harken, B. W. Robertson, and J. I. Brand, *Mater. Sci. Eng. B* **135** (2006), p. 129.

[23] K. Osberg, N. Schemm, S. Balkir, J. I. Brand, S. Hallbeck, and P. Dowben, *IEEE Sens. J.* **6** (2006), p. 1531.

[24] I. Ketsman, Ya. B. Losovyj, A. Sokolov, J. Tang, Z. Wang, K. D. Belashchenko, and P. A. Dowben, *Appl. Phys. A: Mater. Sci. Process.* **89** (2007), pp. 489–492.

[25] Ya. B. Losovyj, I. Ketsman, E. Morikawa, Z. Wang, J. Tang, and P. A. Dowben, *Nucl. Instrum. Methods A* **582** (2007), pp. 264–266.

[26] O. Renault, D. Samour, J.-F. Damlencourt, D. Blin, F. Martin, S. Mathon, N. T. Barrett, and P. Besson, *Appl. Phys. Lett.* **81** (2002), p. 3627.

[27] S. Suzer, S. Sayan, M. M. Banaszak Holl, E. Garfunkel, Z. Hussain, and N. M. Hamdan, *J. Vac. Sci. Technol. A* **21** (2003), p. 106.

[28] S. Sayan, T. Emge, E. Garfunkel, X. Zhao, L. Wielunski, R. A. Bartynski, D. Vanderbilt, J. S. Suehle, S. Suzer, and M. M. Banaszak Holl, *J. Appl. Phys.* **96** (2004), p. 7485.

[29] S. Sayan, R. A. Bartynski, X. Zhao, E. P. Gusev, D. Vanderbilt, M. Croft, M. M. Banaszak Holl, and S. Suzer, *Phys. Stat. Sol. B* **241** (2004), p. 2246.

[30] M. Komatsu, R. Yasuhara, H. Takahashi, S. Toyoda, H. Kumigashira, M. Oshima, D. Kukuruznyak, and T. Chikyow, *Appl. Phys. Lett.* **89** (2006), p. 172107.

[31] P. A. Dowben, D. Li, J. Zhang, and M. Onellion, *J. Vac. Sci. Technol. A* **13** (1995), p. 1549.

[32] T. Kachel, R. Rochow, W. Gudat, R. Jungblut, O. Rader, and C. Cabone, *Phys. Rev. B* **45** (1992), p. 7276.

[33] R. F. Sabirianov, W. N. Mei, J. Lu, Y. Gao, X. C. Zeng, R. D. Bolskar, P. Jeppson, N. Wu, A. N. Caruso, and P. A. Dowben, *J. Phys.: Cond. Matter* **19** (2007), p. 082201.

[34] A. Eichler and G. Kresse, *Phys. Rev. B* **69** (2004), p. 045402.

[35] N. V. Skorodumova, M. Baudin, and K. Hermansson, *Phys. Rev. B* **69** (2004), p. 075401.

[36] J. Uher, S. Pospisil, V. Linhart, and M. Schieber, *Appl. Phys. Lett.* **90** (2007), p. 124101.

[37] S. Balaz, D. I. Dimov, N. M. Boag, K. Nelson, B. Montag, J. I. Brand, and P. A. Dowben, *Appl. Phys. A* **84** (2006), p. 149.

[38] B. W. Robertson, S. Adenwalla, A. Harken, P. Welsch, J. I. Brand, P. A. Dowben, and J. P. Claassen, *Appl. Phys. Lett.* **80** (2002), p. 3644.

[39] S. Adenwalla, P. Welsch, A. Harken, J. I. Brand, A. Sezer, and B.W. Robertson, *Appl. Phys. Lett.* **79** (2001), p. 4357.

[40] T. Aoyama, Y. Oka, K. Honda, and C. Mori, *Nucl. Instrum. Methods Phys. Res. A* **314** (1992), p. 590.